Journal of Energy Storage 66 (2023) 107480

Contents lists available at ScienceDirect

Journal of Energy Storage

journal homepage: www.elsevier.com/locate/est

Research papers

Film processing of Li_6PS_5Cl electrolyte using different binders and their combinations

Artur Tron [a], Raad Hamid [a], Ningxin Zhang [a], Andrea Paolella [a], Paul Wulfert-Holzmann [b], Vladislav Kolotygin [c], Pedro López-Aranguren [c], Alexander Beutl [a,*]

[a] AIT Austrian Institute of Technology GmbH Center for Low-Emission Transport, Battery Technologies, Giefinggasse 2, 1210 Vienna, Austria
[b] Fraunhofer Institute for Surface Engineering and Thin Films IST, Bienroder Weg 54e, 38108 Braunschweig, Germany
[c] Centro de Investigación Cooperativa de Energías Alternativas (CIC energiGUNE) Basque Research and Technology Alliance (BRTA), Parque Tecnológico de Álava Albert Einstein 48, 01510 Vitoria-Gasteiz, Spain

ARTICLE INFO

Keywords:
Li6PS5Cl
Argyrodite
All-solid-state battery
Processing of sulfide electrolytes

ABSTRACT

The development of solid electrolytes has made significant progress in the last decade. Among the most promising materials, sulfide-based electrolytes show high ionic conductivities and low densities, and their precursors are abundant. For industrially relevant battery cells, sulfide electrolytes need to be processed to form thin electrolyte sheets that are either directly applied to the electrodes as coatings or prepared as stand-alone films. Thus, processing of sulfide electrolyte powders has recently drawn much attention as it seems to be one of the major challenges in realizing sulfide-based all-solid-state batteries.

In this work, six different binders (NBR, HNBR, PIB, PBMA, SBS, SEBS) were selected for preparation of electrolyte films using Li_6PS_5Cl as a sulfidic model compound. The influence of the binders on the electrochemical performance as well as on the mechanical properties of the resulting films was investigated. In addition, binder blends were explored as a vial approach to optimize the properties of the electrolyte films. Special focus was put on elucidating the relation between the physico-chemical properties of the binder materials and the resulting electrochemical and mechanical properties of the electrolyte films.

1. Introduction

Significant improvements have been achieved over the last few decades [1] in the development of solid electrolytes for lithium (ion) batteries. Sulfide electrolytes like Li_3PS_4, argyrodites (Li_6PS_5X; X = Cl, Br, I), or Li_2S-P_2S_5 glasses achieve ionic conductivities in the order of 10^{-3} S cm^{-1} close to the ones of their liquid counterparts [2]. In addition, much higher Li^+ transference numbers (around 1 [3], compared to 0.3 for liquid electrolyte [4]) are observed for this class of electrolytes. Nevertheless, battery cells incorporating solid sulfide electrolytes usually show lower performance than comparable systems using liquid electrolytes [5]. Furthermore, elevated pressures need to be applied during battery assembly and operation to ensure good contact between the active material and electrolyte particles [6].

Therefore, the question arises whether and how it is possible to obtain similarly or even higher-performing cells using sulfide electrolytes. In recent years, a lot of research was dedicated to the optimization of sulfide electrolyte processing, especially the argyrodite family [7–10]. The argyrodites show improved performance over other sulfide systems as they achieve high ionic conductivities and form electronically isolating interphases at the Li|electrolyte interface [2], making them kinetically stable components. Ionic conductivities of around 10^{-3} S cm^{-1} can be achieved, and their mechanical properties allow cold-forming processes, in contrast to most oxide-ceramic electrolytes which need high temperatures for compact sintering [11]. Large-scale manufacturing of a mechanically stable film with sufficient ionic conductivity from the precursor sulfide electrolyte powders, however, remains a challenge.

Recently, dry processing of battery materials has become a trend to avoid the use of toxic and hazardous solvents [12]. However, most of the applied processes are difficult to scale to industrially relevant sizes and are not compatible with current battery manufacturing processes. Developing and integrating new production methods means higher costs for the final product. Therefore, an intermediate approach exploits the well-established wet processing technologies of conventional lithium ion batteries [11].

* Corresponding author.
E-mail address: Alexander.beutl@ait.ac.at (A. Beutl).

https://doi.org/10.1016/j.est.2023.107480
Received 31 January 2023; Received in revised form 20 March 2023; Accepted 16 April 2023
Available online 29 April 2023

Electrolyte film preparation using wet processing heavily relies on the selection of a suitable binder material to maintain high cohesion of the electrolyte particles and allows for mechanically demanding processing steps like cutting and rolling. In addition, the selected binder material limits the range of solvents suitable for processing. Although a vast range of different binder materials has been used in literature for argyrodite materials, comparative studies are rare and often restrict their investigations to one-component binder systems [10].

Therefore, in this work we compare different binders and their effect on the ionic conductivity of Li_6PS_5Cl films processed by wet chemical means using tape casting. The impact on the ionic conductivity and processability of the resulting films is evaluated by means of electrochemical impedance spectroscopy and Mandrel bend testing. Furthermore, the effect of binder blends on the performance of the electrolyte films is evaluated. Finally, some considerations for a more efficient approach to binder selection for sulfide-based electrolyte film processing are given.

2. Experimental

2.1. Materials and solvents

Commercially available Li_6PS_5Cl powder was purchased from *NEI Corp.* and used as received. Poly(acrylonitrile-*co*- butadiene), i.e. nitrile butadiene rubber (NBR, Perbunan 1846F, *Arlanxeo*), Hydrated Poly (acrylonitrile-co- butadiene) (HNBR, Therban LT1707, *Arlanxeo*), Polyisobutylene (PIB, OPPANOL N80, *BASF*, Mw ~800,000), Poly(styrene-butadiene-styrene) (SBS, *Sigma-Aldrich*, Mw ~153,000–185,000), Poly (styrene-ethylene-butadiene-styrene) (SEBS, *Sigma-Aldrich*, Mw ~89,000), and Poly(butyl methacrylate) (PBMA, *Sigma-Aldrich*, Mw ~211,000) were used as binder materials and dried at 60C under vacuum for 24 h before usage. Anhydrous p-xylene (Sigma Aldrich) was used as received and was employed as solvent for all binders.

2.2. Processing and manufacturing of electrolyte films

Electrolyte films were prepared as follows. First, binder solutions with different concentrations (NBR – 8 wt%; HNBR – 8 wt%; PIB – 8 wt %; SBS – 16 wt%; SEBS – 16 wt%; PBMA – 20 wt%) were prepared. Appropriate amounts of the binders were dissolved at room temperature using a magnetic stirrer and a glass-covered stirring bar. Higher concentrations were used if the binders did not significantly increase the viscosity of the obtained solutions compared to the pristine solvent at a concentration of 8 wt%. This was necessary to reach similar viscosities for the final electrolyte slurries for all samples. Although the viscosity of the slurries was not measured, it could be qualitatively determined during casting of the samples. The obtained binder solutions were then used for electrolyte film preparation. Appropriate amounts of the electrolyte (usually around 1 g) and binder solutions (usually in the range of 0.2–0.5 g) were mixed in polypropylene pots inside an Ar-filled glovebox (O_2, $H_2O \leq 0.1$ ppm). Additional solvent was added to adjust the solid content. The polypropylene pots were sealed using parafilm© and tape. They were then shuttled outside the glovebox and mixed in a planetary centrifugal mixer (THINKY ARE250) for 3 min at 2000 rpm and for another 2 min at 1000 rpm (degassing step). After transferring back into the glovebox, the obtained slurries were cast onto PTFE foils (thickness = 50 μm, *High-tech-flon*®) using a 200–300 μm doctor blade at shear velocities of 5 mm/s (TFC-200, *automatic research*). The cast films were further dried at room temperature in an inert atmosphere for at least 24 h and further peeled off from the substrate. Samples which could not be peeled off as self-standing films were scratched off from the substrate using a scalpel.

2.3. Powder X-ray diffraction and Scanning electron microscopy

Powder X-ray diffraction (XRD) measurements were conducted using a PANalytical X'Pert Pro in Bragg-Brentano geometry. The X-ray source was a Cu tube using a Ni filter. All samples were prepared in an Ar-filled glovebox and sealed within a sample holder using a polymer cap to avoid any contamination of the samples during the measurements. To limit contamination of the samples with moisture, the measurement time was limited to 1 h and only a limited 2θ range of 5–80° was scanned. The polymer cap shows a broad peak around 20° 2θ, which can be observed in all diffraction patterns.

Scanning electron microscopy (SEM) was performed using a ZEISS Supra 40 electron microscope. The acceleration voltage was set to 3 kV. The sample films were mounted on sample holders inside an Ar-filled glovebox using Ag-paste. Cross-sections for the samples were manually cut using a scalpel. The samples were then transported to the microscope within a sealed container. The container was opened only for mounting the samples onto the SEM instrument, which exposed them to air for around 30 s. Thus, contamination due to adsorbed moisture from the surrounding air could be limited to a minimum, but not fully prevented.

2.4. Electrochemical and mechanical testing

The electrolyte films and powders were tested in a setup described in more detail in [13]. The electrolyte was sandwiched between two steel dies within a polyetherether ketone (PEEK) liner/template (16 mm diameter) and densified by applying 300 MPa for 5 mins. Then the pressure was released, and the impedance was measured at different pressures ranging from 0 to 300 MPa. Frequencies from 1 MHz to 1 Hz were applied using an AC excitation voltage of 10 mV in potentiostatic electrochemical impedance spectroscopy (PEIS) mode. The ionic conductivity was calculated using the following equation, $\sigma = \frac{1}{R} \bullet \frac{l}{A}$ where R is the experimentally determined resistance, while l and A correspond to the electrolyte thickness and area, respectively. An *AMETEK* VersaSTAT MC or *Gamry* Interface 1010E potentiostat was used for all measurements.

Mechanical tests were performed by winding the cast electrolyte films with the PTFE substrate around PTFE cylinders with different diameters in a so-called Mandrel bend test. Thus, strains of 0–4 % were applied, depending on the thickness of the cast samples and the diameter of the PTFE cylinders. The following diameters were selected for the cylinders: 76.20 mm, 25.07 mm, 15.40 mm, 10.30 mm, 7.51 mm, 5.10 mm, 3.25 mm. All samples were optically investigated for cracks or tears after each bending test, which would indicate breakdown of the films.

3. Results and discussion

3.1. Selection of suitable binder materials and solvents for processing

Binders for electrolyte film fabrication using Li_6PS_5Cl need to meet many different requirements. They should be soluble in solvents compatible with the solid electrolyte and should not have an adverse impact on the ionic conductivity. Furthermore, they need to yield sufficiently high mechanical strength to hold particles together and enable processing of the films with established methods like roll-to-roll processes and die-cutting.

Six different binders were investigated for their suitability to be used in combination with the Li_6PS_5Cl material. They are listed in Table 1, and their chemical structures are shown in Fig. S1. NBR and HNBR are random *co*-polymers which have been frequently used as binders for sulfide-based electrolytes [9,10,14,15] due to their compatibility with suitable solvents. HNBR is a derivative of NBR and shows higher oxidative stability due to the elimination of the C=C double bond in the polymer backbone by hydration [16]. SBS and SEBS are *block-co*-polymers with styrene and butadiene blocks aligned in the polymer chains. These blocks form micro-domains of polystyrene (high T_g) which are embedded in a polybutadiene matrix (low T_g) [17]. SEBS is a hydrated derivative of SBS and thus increased oxidative stability is expected

Table 1
Selected binders for processing Li_6PS_5Cl electrolyte films.

Abbreviation	Material	Density [g cm^{-3}]	Average Mw [g mol^{-1}]	T_g [°C]	Product name	Company
NBR	Poly(acrylonitrile-co- butadiene)	0.93	320,000	−30 [18]	Perbunan 1846F, Arlanxeo	Arlanxeo
HNBR	Hydrated Poly(acrylonitrile-co-butadiene)	0.96	542,000	−30 [18]	Therban LT1707, Arlanxeo	Arlanxeo
PIB	Polyisobutylene	0.92	800,000	−64 (from data sheet)	OPPANOL N80, BASF	BASF
PBMA	Poly(butyl methacrylate)	1.07	211,000	20 [19]	Sigma Aldrich	Sigma Aldrich
SBS	Poly(styrene-butadiene-styrene)	0.94	169,000	−25/77 [20]	Sigma Aldrich	Sigma Aldrich
SEBS	Poly(styrene-ethylene-butadiene-styrene)	0.91	89,000	−44/90 [21]	Sigma Aldrich	Sigma Aldrich

(similar to HNBR). Finally, PIB and PBMA are homopolymers which are composed of only one monomer unit. PIB has the lowest and PBMA the highest glass transition temperature (T_g) among the investigated materials, i.e. −64 °C and 20 °C respectively.

First, the solubility of the six binders in the selected solvent, i.e. *p*-xylene, was determined. 6 wt% solutions of all binder-solvent combinations were prepared, and the solubility was optically determined. A good solubility of all binders in *p*-xylene could be observed (cf. Fig. S3), in accordance with literature [7,9,10,14,22,23].

The binder materials were tested for their suitability to prepare freestanding electrolyte films with high ionic conductivities. As previously reported in the literature [10], a binder content of around 3 wt %/5 vol% is sufficient to obtain self-supporting films without deteriorating the ionic conductivity too much.

Furthermore, a solid content of around 54 wt% [9] for the sulfidic electrolyte was assumed to yield an optimized slurry viscosity and rheological behavior for casting. Unfortunately, addition of the different binders to the electrolyte slurries yielded very different viscosities. Although it was possible to cast all samples onto PTFE foils, the quality of the castings varied widely due to the different thickening properties of the binder materials and consequently the different rheological properties of the obtained slurries. Thus, it was decided to vary the solid content by binder in order to obtain similar qualities of the casts.

Freestanding films without any tears or cracks could be obtained for almost all samples, i.e. those containing NBR, HNBR, PBMA, SBS, and SEBS. The electrolyte film obtained from PIB adhered quite strongly to the substrate and could only be removed using a scalpel, however, some cracks could not be avoided during this procedure.

XRD patterns of all prepared electrolyte films were recorded to check for possible incompatibilities. No additional diffraction peaks stemming from decomposition products like LiCl or Li_2S [24,25] could be observed, though (cf. Fig. S2).

3.2. Evaluation of electrochemical properties

The ionic conductivities of the obtained films were measured by PEIS at different pressures. Before the measurements, the samples underwent two different pre-treatments. Sample films labelled as *powdered* were first manually powdered using an agate mortar and further densified into pellets (16 mm diameter; ~1000 µm thickness) applying 300 MPa for 5 min (54MP150D Maassen GmbH). Samples labelled as *film* were only cut into circular shapes (15 mm diameter; ~100 µm thickness) and densified at 300 MPa for 5 min. All measured ionic conductivities are presented in Fig. 1.

A slight difference could be observed when comparing data obtained from the densified electrolyte films and the powdered samples. For most samples (except those using HNBR and PIB) the powdered pellets showed higher ionic conductivities. It is assumed that inhomogeneities in the film thickness were the main reason for this observation, as reported elsewhere [7]. Inhomogeneous material distributions and consequently inhomogeneous thicknesses of the prepared electrolyte films could lead to local differences in the applied pressure and subsequently in the local densities of the samples. For the powdered samples, a more uniform material distribution is to be expected, and thus a more homogenous densification can be achieved (cf. Fig. 2). The ionic conductivity obtained from the PEIS measurements gives the average ionic conductivity of the samples. Thus, areas with low density will give lower ionic conductivities. In contrast, areas with increased density will yield higher conductivity. However, at high pressures, the increase in ionic conductivity becomes less prominent as it can be seen in the pressure dependency of the obtained ionic conductivities in Fig. 1. Therefore, the contribution of the areas with lower density will have a far higher impact on the overall ionic conductivity than areas with higher density, yielding overall lower ionic conductivities for the densified films with inhomogeneous local densities compared to the densified powders.

SEM micrographs of the prepared samples (before densification) show that indeed a high surface roughness is obtained for the cast films, especially at the surface not facing the PTFE substrate. Furthermore, the densified films appeared to be much less homogeneous than the pressed powder pellets, and dark spots could be observed, indicating areas of high densification, see Fig. 3.

Therefore, only measurements of the powdered samples will be compared henceforth for evaluation of the different binder materials so that only the influence of the binder on the ionic conductivity is regarded, uninfluenced by inhomogeneous material distributions.

A comparison of the ionic conductivities obtained from samples using different binders is shown in Fig. 4. The ionic conductivities of all samples increased considerably when the applied pressure was raised from 0 to 50 MPa and reached a plateau at higher pressures (150–300 MPa). It is assumed that contact issues between the electrodes and the electrolyte as well as between the particles are the main cause for the relatively low ionic conductivities observed at lower pressures [6]. Therefore, ionic conductivity values around 100 MPa are used to compare the performance of the different electrolyte films as these are considered to be more reliable. It is reported that carbon electrodes could be used alternatively to improve contact during ionic conductivity measurements of solid-state electrolytes [6].

Samples prepared with PIB and PBMA binders show the highest ionic conductivities at 100 MPa, i.e. $1.24\bullet10^{-3}$ S cm^{-1} and $1.45\bullet10^{-3}$ S cm^{-1}, close to the value of the pristine Li_6PS_5Cl material ($2.14\bullet10^{-3}$ S cm^{-1}). Samples using SEBS and SBS show intermediate ionic conductivities ($1.19\bullet10^{-3}$ and $9.97\bullet10^{-4}$ S cm^{-1}), whereas lowest ionic conductivities are obtained using NBR and HNBR binders ($5.84\bullet10^{-4}$ and $5.80\bullet10^{-4}$ S cm^{-1}).

The data presented in Fig. 4b show the impedance responses of the different samples at 100 MPa. For the pristine Li_6PS_5Cl material a slightly sloped vertical line is obtained, which can be readily fitted assuming an equivalent circuit of R1 + R2/Q2 + Q1; with R1, R2 indicating the bulk and grain boundary resistances and Q1, Q2 constant phase elements assigned to the geometric and double layer capacitances. Samples with PIB, PBMA, SBS and SEBS binders show the same shape as the pristine material, the data is only shifted to higher Z_{Re} values. Addition of a binder material to the electrolyte film reduces the effective electrolyte-electrolyte contact area as some parts of the electrolyte particles are covered with the insulating binder. Thus, higher impedance values are obtained for the composite layers as the tortuosity of the electrolyte film increases. Similar findings were reported elsewhere [26]. For samples using NBR and HNBR, however, an additional semi-

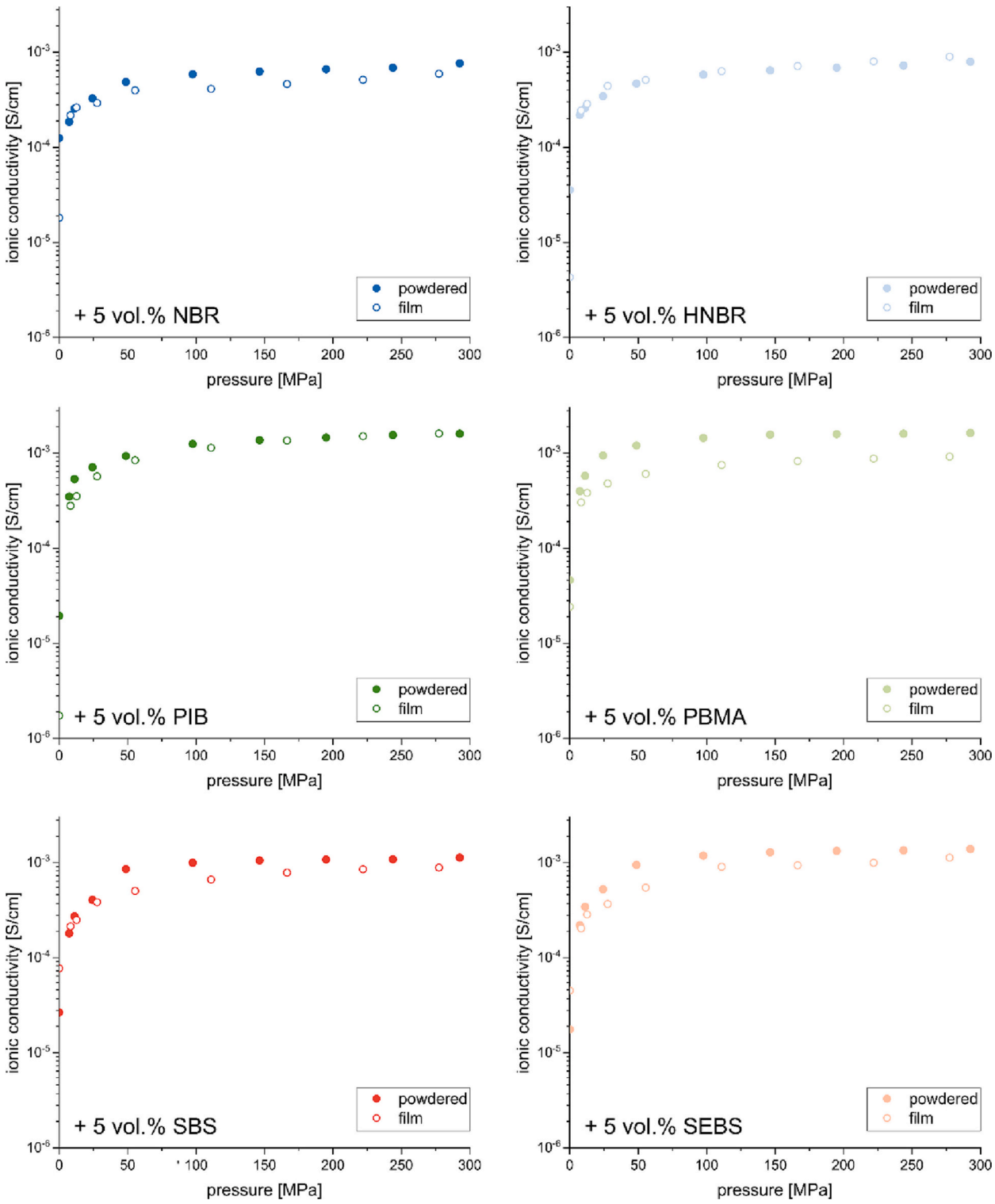

Fig. 1. Ionic conductivity vs. pressure plots of electrolyte films using different binder materials. Black dots show data obtained from densified films, whereas circles show data obtained from densified powdered films.

circle is observed in the Nyquist plots, indicating an additional contribution to the overall impedance of the electrolyte films, which leads to far lower ionic conductivities obtained for samples using these binders. Nevertheless, a recent study showed that stable cycling of NMC811 cells is still possible, even with electrolyte films incorporating 3 wt% of NBR [27].

3.2.1. *SEM micrographs*

SEM micrographs of all samples were recorded, see Figs. S4–S9. Cross-sections and surface morphologies are shown for the as-cast films (i.e. right after drying of the films), and after densification at 300 MPa for 5 min. All films show thicknesses of around 200–150 µm after casting and around 120–90 µm after densification. Large particles stretch almost along the entire thickness of the electrolyte films for some samples, limiting the minimum thickness of the prepared films to around 100 µm.

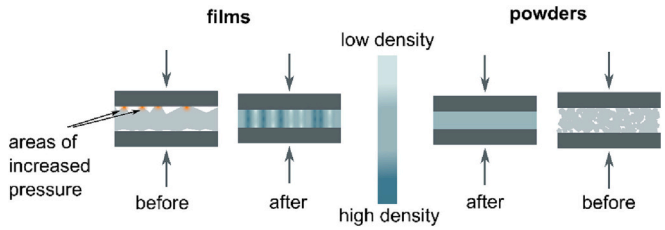

Fig. 2. Schematic outline of densification process of electrolyte films and powdered samples.

In order to prepare even thinner samples, the Li_6PS_5Cl material needs to be crushed by e.g. ball-milling to reduce particle size. However, it is reported that such mechanical treatment can have a negative effect on the specific ionic conductivity of the material [7].

The top side of the films shows rough surfaces, whereas the substrate sides are smooth and pores are readily visible. After densification, however, most of the pores are absent and dense electrolyte layers are obtained. For samples using different binder materials, the obtained porosities of the non-densified films were quite different. For PBMA and SBS containing samples, only low numbers of pores were visible in the SEM micrographs compared to the other samples. During drying of the cast electrolyte films, the used solvent evaporates and leaves pores inside the remaining material. Depending on the amount of solvent used for the electrolyte slurries (i.e. the solid content) a higher or lower degree of porosity can be expected. For longer polymer chains (higher $Mw_{avg.}$) and materials with a high thickening effect, only low solid contents can be achieved, whereas for shorter chains and materials with a low thickening effect, higher solid contents are achievable and thus low porosity films can be prepared.

To further demonstrate the relation between the solid content of the prepared slurries and the porosity of the cast electrolyte films, densities of the as-cast samples were determined. Circular shapes of 16 mm diameter were cut from the films and the thickness was measured using a micrometer screw gauge. Then the weight of each sample piece was measured, and the densities calculated accordingly. These were compared with the solid content of the slurries used for casting. The results are summarized in Fig. 5. A direct relation between the two properties is readily apparent. PBMA and SBS did not significantly increase the viscosity of the electrolyte slurries and thus high solid contents had to be used for slurry preparation. In contrast, HNBR and PIB showed strong thickening effects and thus only low solid contents could be used. The resulting films of electrolyte slurries using high solid contents also show low porosities and densities close to the value of pristine Li_6PS_5Cl, i.e. 1.64 g cm^{-3} [28], even without densification of the films. In contrast, films prepared using slurries with low solid contents resulted in films with high porosity and thus low densities. After densification by

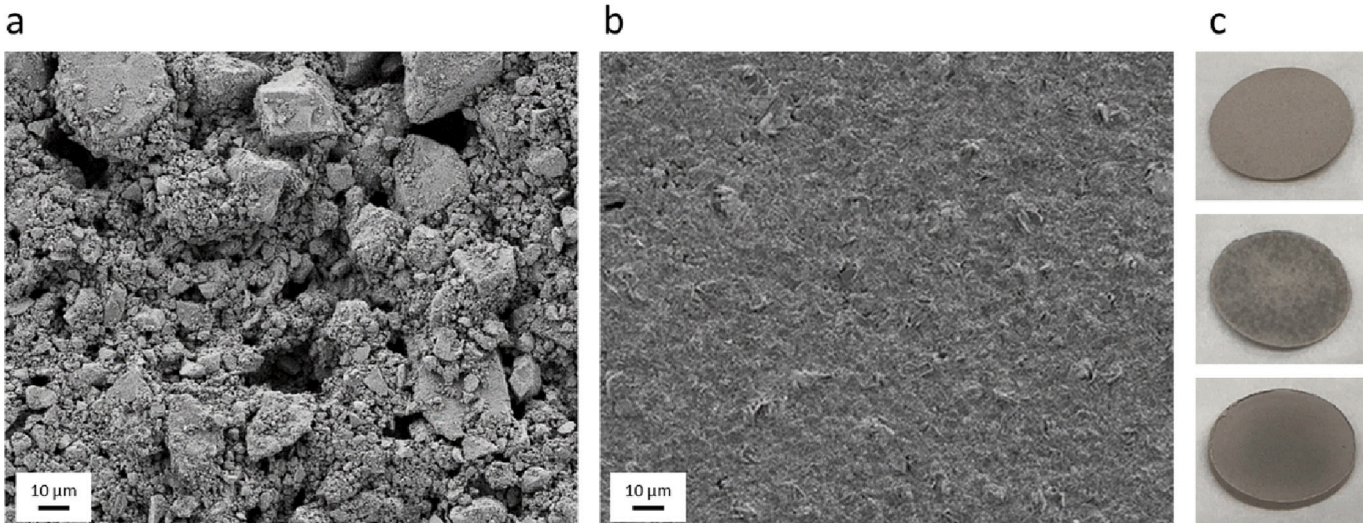

Fig. 3. As-cast electrolyte film prepared using HNBR as binder material. a, SEM micrograph of top surface of as-cast electrolyte; b, SEM micrograph of top surface of densified electrolyte; c, optical images of the as cast film (top), densified film (middle), and densified powder pellet (bottom).

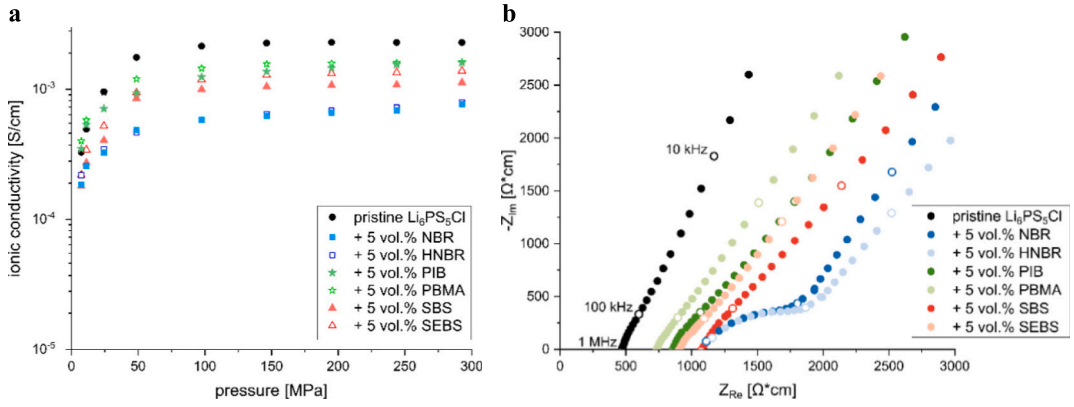

Fig. 4. a, ionic conductivity vs. pressure plots of samples using different binder materials; b, corresponding PEIS signals obtained at 100 MPa (open symbols indicate frequencies – every decade).

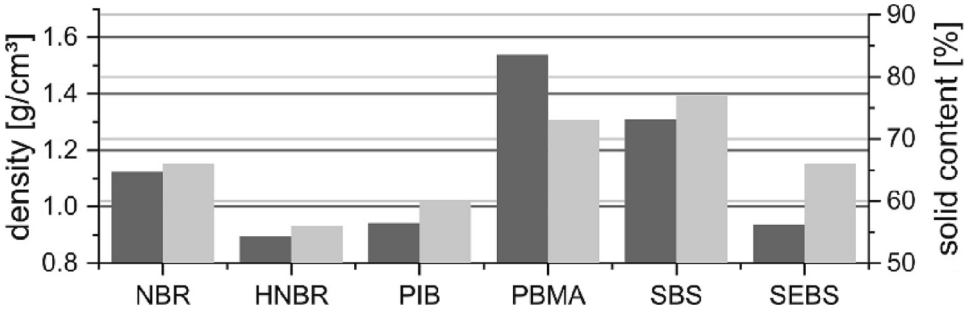

Fig. 5. Densities (dark bars) of as-cast electrolyte films and solid contents (light bars) of the corresponding slurries using different binder materials.

uniaxial pressing of the sample films, though, densities close the theoretical one were found for all samples.

3.3. Mechanical stability of electrolyte films

For industrially relevant production technologies, like roll-to-roll processes or die cutting, the mechanical flexibility and coherence of the films are of significant importance. Therefore, the mechanical stability of the electrolyte films incorporating different binder materials was evaluated using Mandrel bend testing. The cast films were bent over PTFE cylinders with different radii R and the maximum applied strain on the surface of the films calculated according to $\varepsilon = \frac{d_f + d_{sub}}{2R}$ [29], where d_f and d_{sub} are the thicknesses of the films and substrates, respectively.

The results are summarized in Table 2 and Figs. S10–S15.

The electrolyte films using NBR, HNBR and PIB did not break during the measurements. They showed good flexibility and low stiffness, easily sustaining strains around 3 %. Films prepared using SBS and SEBS showed similar behavior up to strains of 2–2.5 %. However, after bending the films around the 3.25 mm cylinder, strains of 2.69 % and 3.99 % were applied, which resulted in breakdown of the films. The highest stiffness and least flexibility were observed for the sample using PBMA as binder. The film could not sustain strains of around 0.86 % and broke along the whole film width. The glass transition temperatures for the different binder materials seem to be a good indicator for the resulting flexibility of the electrolyte films. NBR, HNBR and PIB have low T_g values of < -30 °C. Due to the high mobility of the polymer chains at room temperature, the electrolyte films using these materials as binder show high flexibility. In contrast, PBMA with T_g lying at around 20 °C, the polymer chains are rather stiff, and their mobility is limited. Therefore, the resulting electrolyte film is stiff as well, showing only low flexibility. For SBS and SEBS, intermediate flexibility was observed. Both of these binders are composed of two immiscible domains with high and low T_g values [20,21]. Thus, overall medium flexibility is observed for electrolyte films using these binders.

Some differences in the adhesion of the electrolyte films on the PTFE substrate as well as in the cohesion of the films were also observed, although not quantified. It seems that samples using NBR, and PBMA had low adhesive strength on the PTFE substrate, and high cohesion. Therefore, lifting off the films from the substrate did not cause any problems. Samples with HNBR, SBS, and SEBS adhered more strongly to the substrate and showed lower cohesion compared to the sample using e.g. NBR. Thus, they had to be carefully removed from the substrate to avoid any tearing or cracking by detaching them step by step from the PTFE substrate using a scalpel. The sample using PIB adhered the strongest and showed the lowest cohesion. Consequently, removal from the substrate was only possible by scratching/scraping the film off the substrate. During this procedure, tearing and cracking of the film could not be avoided.

3.4. Binder composites

The properties of the Li_6PS_5Cl electrolyte films using different binder materials are summarized in Table 3. It can be seen that none of the prepared electrolyte films show both high ionic conductivity combined with good mechanical performance and processability. Films prepared using NBR and HNBR are highly flexible with good processability. However, an additional contribution to electrolyte impedance could be observed, reducing the ionic conductivities to low values of around $5 \bullet 10^{-4}$ S cm^{-1}. Furthermore, both binders lead to rather high viscosities of the electrolyte slurries and thus relatively low solid contents can be achieved. Consequently, high initial porosities are obtained for the prepared electrolyte films. For films prepared using PIB, high ionic conductivities and high flexibility can be achieved. Nevertheless, strong adhesion to the substrate and low cohesion renders handling of the films difficult. Similarly, to NBR and HNBR, PIB increases the viscosity of the electrolyte slurry significantly and thus only low solid contents can be realized. PBMA yields highly ionic conductive films, which are rather stiff and easily crack during cutting or bending. Nevertheless, high solid contents are possible due to the low thickening effect of PBMA in p-xylene, and thus low initial porosities can be obtained. SBS and SEBS perform similarly and yield balanced properties. The ionic conductivities are not as high as for films using PIB and PBMA and not as low as for NBR and HNBR. The mechanical flexibility is sufficient for properly handling the films, but not as high as for NBR, HNBR and PIB. The cohesive and adhesive properties are also acceptable, and handling of the films seems adequate for processing.

In order to balance the ionic conductivities with the mechanical properties of the electrolyte films, binder composites were considered.

Table 2
Results of Mandrel bend testing of electrolyte films using different binder materials. The applied strain ε is calculated from the film and substrate thicknesses d_f and d_{sub}. Mechanical film failure is indicated by bold numbers.

Mandrel radius [mm]			76.20	25.07	15.40	10.30	7.51	5.10	3.25
Binder	d_f [µm]	d_{sub} [µm]	Strain [%]						
NBR	148	50	0.13	0.39	0.64	0.95	1.30	1.90	2.96
HNBR	129	50	0.12	0.36	0.58	0.86	1.18	1.72	2.68
PIB	158	50	0.14	0.41	0.67	1.00	1.37	2.00	3.10
PBMA	129	50	0.12	0.36	0.58	**0.86**			
SBS	130	50	0.12	0.36	0.58	0.87	1.18	1.73	**2.69**
SEBS	220	50	0.18	0.54	0.87	1.29	1.77	2.58	**3.99**

Table 3
Properties of Li_6PS_5Cl films as determined in this study. Additionally, the solid contents of the slurries used for casting are given.

Binder	Adhesion to PTFE substrate	Flexibilty of film	Cohesive properties	Solid content of slurry [wt %]	Porosity of as-cast films [%]	Ionic conductivity at 100 MPa [S cm^{-1}]
NBR	Low	High	High	66	31	$5.84•10^{-4}$
HNBR	Low	High	High	56	45	$5.80•10^{-4}$
PIB	High	High	Very low	60	43	$1.24•10^{-3}$
PBMA	Very low	Very low	Low	73	6	$1.45•10^{-3}$
SBS	Low	Medium	Medium	77	20	$9.97•10^{-4}$
SEBS	Medium	Medium	Medium	66	42	$1.19•10^{-3}$

The binder yielding the best mechanical performance, NBR, was mixed with the two binders showing the highest ionic conductivities, PIB/PBMA, at different ratios. Furthermore, PIB and PBMA were also mixed to maintain high ionic conductivities and compensate for the stiffness of PBMA and the high adhesion on the substrate as well as the low cohesion of PIB. Ionic conductivity measurements were conducted in the same way as for the single-binder samples and are presented in Fig. 6. Furthermore, the flexibility of the films was tested by Mandrel bend test. The results are summarized in Table 4.

Addition of PBMA to electrolyte films using NBR binder increased the achievable ionic conductivities. Conductivity values of $7.62•10^{-4}$ S cm^{-1} and $9.88•10^{-4}$ S cm^{-1} were obtained for binder ratios of PBMA:NBR = 1:2 and 2:1 (vol./vol.), respectively. On the other hand, the mechanical stability decreased. At a PBMA:NBR ratio of 1:2, the electrolyte film can endure >3.5 % of strain, whereas the film using a ratio of 2:1 broke down at strains of 1.8 %.

For PIB + NBR blends, the ionic conductivity did not change much upon addition of low amounts of PIB in a PIB:NBR ratio of 1:2. Only addition of more PIB (PIB:NBR = 2:1) increased the ionic conductivities significantly to values of $7.41•10^{-4}$ S cm^{-1}. Good flexibility was obtained for both ratios - they easily sustain strains of around 3 % without cracking. Nevertheless, some issues regarding the removal of the films from the substrate remained. It was only possible to remove the sample using a binder ratio of PIB:NBR = 1:2 without any tearing. For the sample using a higher amount of PIB, i.e. PIB:NBR = 2:1, the electrolyte film adhered too strongly to the substrate and similarly to the sample using only PIB, the electrolyte film could only be removed by scraping with a scalpel.

For the PIB + PBMA blends, no significant difference in the ionic conductivities could be observed for the different blend ratios. This is to be expected from the similar ionic conductivities obtained for films using either of the two binder materials. However, the flexibility of the films could be improved compared to films using only PBMA. Films using a binder ratio of PIB:PBMA = 1:2 broke down at a strain of 2.64 %, whereas films using a higher amount of PIB (PIB:PBMA = 2:1) did not show any mechanical failure during testing. Hence, a ratio of PIB:PBMA of 2:1 seems preferable. Thus, it seems that PIB is more potent in reducing crack formation when mixed with PBMA compared to NBR + PBMA blends. In contrast, though, electrolyte films including NBR can be removed from the substrate more easily and showed better cohesive properties.

4. Discussion

The selection of a suitable binder material for sulfide-based electrolytes has been done mainly on a trial-and-error base up until now. Thus, a variety of different polymers have been identified as potential binders for preparation of electrolyte films. In many cases, however, one material cannot meet all the requirements for obtaining both mechanically strong and highly ionically conductive films. Therefore, combinations of two and more binders will be necessary to further optimize the preparation of sulfide-based electrolyte films. In order to enable a more efficient selection of different binder materials, some considerations about the relation between the physico-chemical properties of the investigated materials in this work and the resulting electrochemical and mechanical properties of the prepared films are given in the following below. Nevertheless, more detailed investigations on the different considerations are proposed as they have important implications not only for processing of electrolyte films but also for composite electrodes.

The selected polymers in this work can be classified into three different groups. NBR and HNBR are random *co*-polymers, PIB and PBMA are homopolymers, whereas SBS and SEBS are *block-co*-polymers.

The glass transition temperatures and thus the mobility of the polymeric chains is quite different for the different materials (cf. Table 1). NBR, HNBR and PIB show low T_g values in the range between −30 °C and − 64 °C, whereas PBMA shows values of >20 °C [19,30]. Both high and low T_g values can be found for the different blocks of the *block-co*-polymers, showing values of −25 °C to −44 °C for the butadiene blocks and 77 to 90 °C for the styrene blocks, respectively. The blocks in SBS and SEBS are immiscible, and two domains are formed within the polymer matrix. The hard polystyrene blocks accumulate and form domains within a “soft” polybutadiene rubber matrix [17,31]. Therefore, two values for T_g are given in Table 1 to account for the different

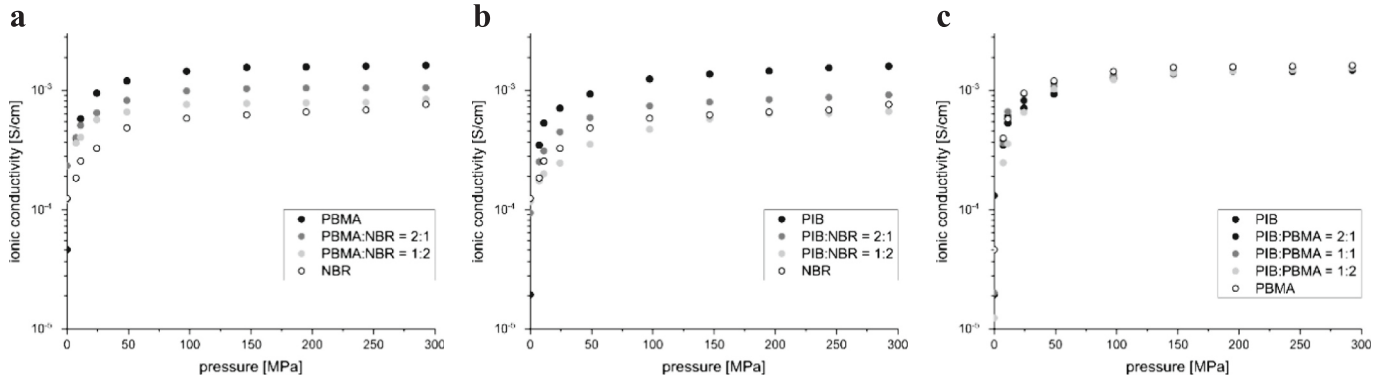

Fig. 6. Pressure dependence of ionic conductivity of different electrolyte films using of binder material blends. a, NBR and PBMA; b, NBR and PIB; c, PIB and PBMA (ratios are given in vol. fraction).

Table 4
Results of Mandrel bend testing of electrolyte films using binder material blends. The applied strain ε is calculated from the film and substrate thicknesses d_f and d_{sub}. Film failure is indicated by bold numbers.

Mandrel radius [mm]			76.20	25.07	15.40	10.30	7.51	5.10	3.25
Binder	d_f [µm]	d_{sub} [µm]	Strain [%]						
PIB:NBR = 2:1	148	50	0.11	0.35	0.56	0.84	1.15	1.69	2.62
PIB:NBR = 1:2	129	50	0.13	0.38	0.62	0.93	1.27	1.86	2.88
PBMA:NBR = 2:1	137	50	0.12	0.37	0.60	0.90	1.23	**1.80**	–
PBMA:NBR = 1:2	188	50	0.16	0.47	0.77	1.14	1.56	2.28	3.53
PIB:PBMA = 2:1	106	50	0.10	0.31	0.50	0.75	1.03	1.51	2.34
PIB:PBMA = 1:2	126	50	0.12	0.35	0.57	0.85	1.16	1.70	**2.64**

behavior of the different domains. The mobility of the polymeric chains for the different binders seem to directly influence the mechanical properties of cast electrolyte films. Samples using binders with low T_g values (NBR, HNBR, and PIB) showed good flexibility, whereas samples using binders with high T_g (PBMA) showed brittle behavior. Furthermore, samples using SBS and SEBS, which exhibit domains with high and low T_g, show intermediate flexibilities. Thus, the T_g value of binder materials can be used as a good indicator for the resulting flexibility of the prepared electrolyte films.

Apart from T_g, the polarity and dielectric constant of the respective binders are also important parameters for processing. Binder materials with high polarity are expected to have a stronger interaction with the electrolyte particles and can more effectively avoid agglomeration by flocculation than materials with low polarity. The polarities of the binder materials selected for this work are indicated by the polar contribution to the Hansen solubility parameters (cf. Table 5). Polymer binders with polar groups like NBR and HNBR are assumed to form a thin insulating layer around the electrolyte particles, thus leading to an additional contribution in the impedance response. In case of binders with lower polarity like PIB and SBS, electrolyte agglomeration is more probable, and the binder is more likely to remain in between the agglomerates. Thus, ionically conducting percolation paths are less likely to be interrupted by the binder, resulting in higher ionic conductivities. Similar findings were recently discussed in [33].

For PBMA, which shows similar polarities as HNBR, this trend is not observed and no additional contribution to the impedance can be found. To explain this observation, the polymer-solvent interaction needs to be considered. For all binders, p-xylene was used as solvent. The polymer conformation of the dissolved materials heavily depends on the selected solvents. For NBR, HNBR, and PIB a highly viscous solution was obtained after dissolution in p-xylene, indicating a stretched conformation for the polymeric chains. In contrast, dissolution of PBMA in p-xylene did not significantly increase the viscosity of the solution, indicating a coiled conformation of the polymer. Consequently, less area can be covered for the coiled PBMA polymer chains compared to the stretched NBR chains. Therefore, percolation of the electrolyte particles in the cast films is less inhibited by PBMA, leading to higher ionic conductivities compared to NBR. Furthermore, the large n-butyl side chain of PBMA restricts the movement of the dissolved polymer [32], promoting coiled configurations.

Summarizing, one can conclude that due to the relatively high polarity of NBR/HNBR as well as high flexibility of the polymer chains (low T_g) and stretched conformation within the selected p-xylene solvent the electrolyte particles in the prepared films are completely covered with a thin insulating polymer layer. This results not only in an additional contribution to the impedance response, but also in good flexibility and high cohesion of the prepared electrolyte films.

PIB shows similar properties as NBR/HNBR, however, its lower polarity values seem to reduce the interaction of the binder with the electrolyte particles. Thus, agglomeration of electrolyte particles is increased, and the binder remains in gaps and pores of the prepared films. Consequently, high ionic conductivities but low cohesion of the prepared films is observed.

For PBMA, the restricted mobility of the molecular chains due to the bulky n-butyl side group and poor compatibility with the selected solvent promote a coiled configuration of the dissolved polymer. Thus, less area can be covered with the same amount of material, leading to undisturbed percolation networks of the electrolyte particles. The high T_g value, however, leads to brittleness in the processed films.

For SBS and SEBS, the two immiscible blocks of the polymer chains behave quite differently, indicated by the large difference of their respective T_g values. Therefore, the properties of the prepared films using these binders show intermediate ionic conductivity as well as mechanical stability.

To verify these assumptions, a more rigorous study needs to be conducted. This should include the influence of the different binders on the microstructure and especially the porosity of the films to enable a full understanding of the interaction of the binder with the sulfide electrolyte. Due to the complexity of such measurements (cf. [35]), though, this is outside the scope of this work. Furthermore, the temperature dependency of the mechanical properties of the selected binders should be investigated by dynamic mechanical analysis to enable optimization of processing parameters for warm calendering/pressing of the electrolyte films.

Nevertheless, a more fundamental understanding of the binder-electrolyte interaction is assumed to significantly promote the development of all-solid-state batteries using sulfide-electrolytes.

Table 5
Hansen solubility parameter of selected polymer binders [30] and p-xylene solvent [34].

Polymer	Hansen solubility parameter		
	δ_D	δ_P	δ_H
NBR	17.2	8.6	4.3
HNBR	18.4	6.0	4.5
PIB	16.4–16.9	1.7–2.5	4.0–4.7
PBMA	16.0–18.3	4.9–6.2	6.3–6.6
SBS	17.4	1.1	2.6
p-xylene	17.4	1.0	3.1

5. Conclusion

Six different binder materials, NBR, HNBR, PIB, PBMA, SBS, and SEBS, were compared for their suitability to act as binders for Li_6PS_5Cl. The prepared electrolyte films showed different ionic conductivities and mechanical properties. NBR and HNBR binders yield an additional contribution to the impedance of the electrolyte films, and overall lower ionic conductivities were observed compared to samples prepared with the other selected binders. On the other hand, good film flexibility, high cohesion and low adhesion to the PTFE substrate rendered electrolyte films prepared with these materials as the mechanically best performing ones. In contrast, electrolyte films prepared with PIB and PBMA showed the highest ionic conductivities close to that of the pristine Li_6PS_5Cl. For PIB, however, the strong adhesion to the substrate, as well as the low cohesion of the films rendered further processing as freestanding films difficult and it was only possible to scrape the films off the substrate,

leading to cracks and tears. For electrolyte films using PBMA, lifting the film off the substrate was easy due to the low adhesion on the substrate and acceptable cohesion, nevertheless, poor flexibility of the film made it quite brittle and proper cutting of the film was difficult. Electrolyte films using SBS and SEBS showed intermediate performance with ionic conductivities and mechanical properties lying between the ones of films prepared by NBR/HNBR and PIB/PBMA. To compensate for the limitations of single binder systems, binder blends offer a promising method to balance the mechanical and electrochemical performance of electrolyte films.

CRediT authorship contribution statement

Alexander Beutl: Conceptualization, Formal analysis, Investigation, Methodology, Project administration, Supervision, Validation, Visualization, Writing – Original Draft, Writing- Reviewing and Editing. Artur Tron: Investigation, Writing- Reviewing and Editing. Raad Hamid: Investigation. Ningxin Zhang: Investigation. Vladislav Kolotygin: Writing- Reviewing and Editing. Pedro López-Aranguren: Writing- Reviewing and Editing. Paul Wulfert-Holzmann: Writing- Reviewing and Editing.

Declaration of competing interest

- The authors have no relevant financial or non-financial interests to declare.
- The authors have no conflicts of interest to declare that are relevant to the content of this article.
- All authors certify that they have no affiliations with or involvement in any organization or entity with any financial interest or non-financial interest in the subject matter or materials discussed in this manuscript.
- The authors have no financial or proprietary interests in any material discussed in this article.

Data availability

Data will be made available on request.

Acknowledgements

The presented work was supported by the European Commission through the H2020 program under Grant agreement number 875028 (SUBLIME Project). Furthermore, the authors want to express their gratitude to Jacqueline Winter for linguistic proofreading and corrections.

Appendix A. Supplementary data

Supplementary data to this article can be found online at https://doi.org/10.1016/j.est.2023.107480.

References

[1] A.M. Abakumov, S.S. Fedotov, E.V. Antipov, J.-M. Tarascon, Solid state chemistry for developing better metal-ion batteries, Nat. Commun. 11 (2020) 4976, https://doi.org/10.1038/s41467-020-18736-7.
[2] Y.-W. Byeon, H. Kim, Review on interface and interphase issues in sulfide solid-state electrolytes for all-solid-state Li-metal batteries, Electrochem. 2 (2021) 452–471, https://doi.org/10.3390/electrochem2030030.
[3] S. Wang, Y. Zhang, X. Zhang, T. Liu, Y. Lin, Y. Shen, L. Li, C. Nan, High-conductivity argyrodite Li6PS5Cl solid electrolytes prepared via optimized sintering processes for all-solid-state lithium-sulfur batteries, ACS Appl. Mater. Interfaces 10 (2018) 42279–42285, https://doi.org/10.1021/acsami.8b15121.
[4] S. Zugmann, M. Fleischmann, M. Amereller, R.M. Gschwind, H.D. Wiemhöfer, H. J. Gores, Measurement of transference numbers for lithium ion electrolytes via four different methods, a comparative study, Electrochim. Acta 56 (2011) 3926–3933, https://doi.org/10.1016/j.electacta.2011.02.025.
[5] R. Koerver, I. Aygün, T. Leichtweiß, C. Dietrich, W. Zhang, J.O. Binder, P. Hartmann, W.G. Zeier, J. Janek, Capacity fade in solid-state batteries: interphase formation and chemomechanical processes in nickel-rich layered oxide cathodes and lithium thiophosphate solid electrolytes, Chem. Mater. 29 (2017) 5574–5582, https://doi.org/10.1021/acs.chemmater.7b00931.
[6] J.-M. Doux, Y. Yang, D.H.S. Tan, H. Nguyen, E.A. Wu, X. Wang, A. Banerjee, Y. S. Meng, Pressure effects on sulfide electrolytes for all solid-state batteries, J. Mater. Chem. A 8 (2020) 5049, https://doi.org/10.1039/C9TA12889A.
[7] Y.-T. Chen, M. Duquesnoy, D.H.S. Tan, J.-M. Doux, H. Yang, G. Deysher, P. Ridley, A.A. Franco, Y.S. Meng, Z. Chen, Fabrication of high-quality thin solid-state electrolyte films assisted by machine learning, ACS Energy Lett. 6 (2021) 1639–1648, https://doi.org/10.1021/acsenergylett.1c00332.
[8] C. Doerrer, I. Capone, S. Narayanan, J. Liu, C.R.M. Grovenor, M. Pasta, P.S. Grant, High energy density single-crystal NMC/Li6PS5Cl cathodes for all-solid-state lithium-metal batteries, ACS Appl. Mater. Interfaces 13 (2021) 37809–37815, https://doi.org/10.1021/acsami.1c07952.
[9] B. Emley, Y. Liang, R. Chen, C. Wu, M. Pan, Z. Fan, Y. Yao, On the quality of tape-cast thin films of sulfide electrolytes for solid-state batteries, Mater. Today Phys. 18 (2021), 100397, https://doi.org/10.1016/j.mtphys.2021.100397.
[10] N. Riphaus, P. Strobl, B. Stiaszny, T. Zinkevich, M. Yavuz, J. Schnell, S. Indris, H. A. Gasteiger, S.J. Sedlmaier, Slurry-based processing of solid electrolytes: a comparative binder study, J. Electrochem. Soc. 165 (2018) A3993–A3999, https://doi.org/10.1149/2.0961816jes.
[11] J. Schnell, T. Günther, T. Knoche, C. Vieider, L. Köhler, A. Just, M. Keller, S. Passerini, G. Reinhart, All-solid-state lithium-ion and lithium metal batteries – paving the way to large-scale production, J. Power Sources 382 (2018) 160–175, https://doi.org/10.1016/j.jpowsour.2018.02.062.
[12] N. Verdier, G. Foran, D. Lepage, A. Prébé, D. Aymé-Perrot, M. Dollé, Challenges in solvent-free methods for manufacturing electrodes and electrolytes for lithium-based batteries, Polymers 13 (2021) 323, https://doi.org/10.3390/polym13030323.
[13] M. Batzer, K. Voges, W. Wang, P. Michalowski, A. Kwade, Systematic evaluation of materials and recipe for scalable processing of sulfide-based solid-state batteries, Mater. Today Commun. 30 (2022), 103189, https://doi.org/10.1016/j.mtcomm.2022.103189.
[14] Y.J. Nam, D.Y. Oh, S.H. Jung, Y.S. Jung, Toward practical all-solid-state lithium-ion batteries with high energy density and safety: comparative study for electrodes fabricated by dry- and slurry-mixing processes, J. Power Sources 375 (2018) 93–101, https://doi.org/10.1016/j.jpowsour.2017.11.031.
[15] K.T. Kim, D.Y. Oh, S. Jun, Y.B. Song, T.Y. Kwon, Y. Han, Y.S. Jung, Tailoring slurries using cosolvents and Li salt targeting practical all-solid-state batteries employing sulfide solid electrolytes, Adv. Energy Mater. 11 (2021), 2003766, https://doi.org/10.1002/aenm.202003766.
[16] Z. Li, Y. Zhao, W.E. Tenhaeff, 5 V stable nitrile-bearing polymer electrolyte with aliphatic segment as internal plasticizer, ACS Appl. Energy Mater. 2 (2019) 3264–3273, https://doi.org/10.1021/acsaem.9b00103.
[17] S. Basak, A. Bandyopadhyay, Styrene-butadiene-styrene-based shape memory polymers: evolution and the current state of art, Polym. Adv. Technol. 33 (2022) 2091–2112, https://doi.org/10.1002/pat.5682.
[18] J. Liu, J. Sun, Z. Zhang, H. Yang, X. Nie, One-step synthesis of end-functionalized hydrogenated nitrile-butadiene rubber by combining the functional metathesis with hydrogenation, ChemistryOpen 9 (2020) 374–380, https://doi.org/10.1002/open.201900369.
[19] R. Arunkumar, R.S. Babu, M.U. Rani, S. Kalainathan, Effect of PBMA on PVC-based polymer blend electrolytes, J. Appl. Polym. Sci. 134 (2017) 44939, https://doi.org/10.1002/app.44939.
[20] J.-F. Masson, S. Bundalo-Perc, A. Delgado, Glass transitions and mixed phases in block SBS, J. Polym. Sci. B Polym. Phys. 43 (2004) 276–279, https://doi.org/10.1002/polb.20319.
[21] P. Gupta, M. Bera, P.K. Maji, Nanotailoring of sepiolite clay with poly[styrene-b-(ethylene-co-butylene)-b-styrene]: structure–property correlation, Polym. Adv. Technol. 28 (2017) 1428–1437, https://doi.org/10.1002/pat.4019.
[22] D.H.S. Tan, A. Banerjee, Z. Deng, E.A. Wu, H. Nguyen, J.-M. Doux, X. Wang, J.-H. Cheng, S.P. Ong, Y.S. Meng, Z. Chen, Enabling thin and flexible solid-state composite electrolytes by the scalable solution process, ACS Appl. Energy Mater. 2 (2019) 6542–6550, https://doi.org/10.1021/acsaem.9b01111.
[23] Y.-G. Lee, S. Fujiki, C. Jung, N. Suzuki, N. Yashiro, R. Omoda, D.-S. Ko, T. Shiratsuchi, T. Sugimoto, S. Ryu, J.H. Ku, T. Watanabe, Y. Park, Y. Aihara, D. Im, I.T. Han, High-energy long-cycling all-solid-state lithium metal batteries enabled by silver–carbon composite anodes, Nat.Energy 5 (2020) 299–308, https://doi.org/10.1038/s41560-020-0575-z.
[24] J. Ruhl, L.M. Riegger, M. Ghidiu, W.G. Zeier, Impact of solvent treatment of the superionic argyrodite Li6PS5Cl on solid-state battery performance, Adv. Energy Sustain. Res. 2 (2021), 2000077, https://doi.org/10.1002/aesr.202000077.
[25] Z. Zhang, L. Zhang, Y. Liu, X. Yan, B. Xu, L.-M. Wang, One-step solution process toward formation of Li6PS5Cl argyrodite solid electrolyte for all-solid-state lithium-ion batteries, J. Alloys Compd. 812 (2020), 152103, https://doi.org/10.1016/j.jallcom.2019.152103.
[26] S. Wang, X. Zhang, S. Liu, C. Xin, C. Xue, F. Richter, L. Li, L. Fan, Y. Lin, Y. Shen, J. Janek, C.-W. Nan, High-conductivity free-standing Li6PS5Cl/poly(vinylidene difluoride)composite solid electrolyte membranes for lithium-ion batteries, J. Materiomics 6 (2020) 70–76, https://doi.org/10.1016/j.jmat.2019.12.010.
[27] A. Tron, R. Hamid, N. Zhang, A. Beutl, Rational optimization of cathode composites for sulfide-based all-solid-state batteries, Nanomaterials 13 (2023) 327, https://doi.org/10.3390/nano13020327.

[28] Y. Zhou, C. Doerrer, J. Kasemchainan, P.G. Bruce, M. Pasta, L.J. Hardwick, Observation of interfacial degradation of Li6PS5Cl against lithium metal and LiCoO2 via in situ electrochemical Raman microscopy, Batteries Supercaps 3 (2020) 647–652, https://doi.org/10.1002/batt.201900218.
[29] Z. Suo, Mechanics of rollable and foldable film-on-foil electronics, Appl. Phys. Lett. 74 (1999) 1177, https://doi.org/10.1063/1.123478.
[30] G. Wypych, Handbook of Polymers, second ed., ChemTec Publishing, Ontario, 2016.
[31] R. Banerjee, S.S. Ray, A.K. Ghosh, Microstructure development and its influence on the properties of styrene-ethylene-butylene-styrene/polystyrene blends, Polymers 10 (2018) 400, https://doi.org/10.3390/polym10040400.
[32] T. Li, H. Li, H. Wang, W. Lu, M. Osa, Y. Wang, J. Mays, K. Hong, Chain flexibility and glass transition temperatures of poly(n-alkyl (meth)acrylate)s: implications of tacticity and chain dynamics, Polymer 213 (2021), 123207, https://doi.org/10.1016/j.polymer.2020.123207.
[33] Y. Li, D. Zhang, X. Xu, Z. Wang, Z. Liu, J. Shen, J. Liu, M. Zhu, J. Energy Chem. 60 (2021) 32–60, https://doi.org/10.1016/j.jechem.2020.12.017.
[34] C.M. Hansen, Hansen Solubility Parameters, a Users's Handbook, second ed., CRC Press, Boca Raton, 2007.
[35] T. Beuse, M. Fingerle, C. Wagner, M. Winter, M. Börner, Comprehensive insights into the porosity of lithium-ion battery electrodes: a comparative study on positive electrodes based on LiNi0.6Mn0.2Co0.2O2 (NMC622), Batteries 7 (2021) 70, https://doi.org/10.3390/batteries7040070.